Department of Engineering Physics and Mathematics
Helsinki University of Technology
02015 Espoo, Finland

NUCLEAR MAGNETISM AND SUPERCONDUCTIVITY IN RHODIUM

Tauno Knuuttila

Low Temperature Laboratory

Dissertation for the degree of Doctor of Science in Technology to be presented with due permission of the Department of Engineering Physics and Mathematics for public examination and debate in Auditorium F1 at the Helsinki University of Technology (Espoo, Finland) on the 24th of November, at 12 noon.

Espoo 2000

Contents

1 Introduction

Nuclear spins provide excellent model systems for studies of ground state problems in magnetism, as the interactions between the spins are in most cases fairly simple and can be calculated with good precision. Contrary to electronic systems, the nuclei are well localized in their lattice sites and the lattice geometry remains unchanged in the magnetically ordered state due to the small energy scales. However, owing to the smallness of the nuclear magneton, the research of nuclear magnetism is difficult from the experimental point of view. Spontaneous ordering of the nuclear spins can be expected when the thermal energy k_BT becomes comparable with the interaction energy of the spin system, which typically requires temperatures in the microkelvin range or below. This is at least six orders of magnitude lower than that required for electronic magnets. Still, the development of advanced cooling techniques has enabled experiments, where nuclear magnetic ordering can be accessed. Ordered states were first reached in several insulators, CaF_2, LiF and LiH [1] in the early 1970's and only later in pure metals, Cu in 1982 [2] and Ag in 1991 [3].

An interesting aspect of this research is nuclear magnetism in a superconducting host material. The interaction of the nuclear spins with the electron system can provide fundamental information of the superconducting state, as shown already in the late 1950's by Hebel and Slichter [4], whose spin-lattice relaxation measurements in superconducting aluminum provided one of the first convincing proofs supporting the BCS theory of superconductivity. In the past, the interaction between the nuclear spins and electrons in superconductors has been investigated under conditions, where nuclear magnetism is too weak to affect the superconducting properties. Only recently experiments beyond this restriction have been performed at very low temperatures in $AuIn_2$ and Al [5, 6], but in those studies no relaxation measurements were made in the superconducting state.

Rhodium is an excellent candidate for studies of nuclear magnetism and its interaction with superconductivity, as it possesses suitable properties for practical experiments in both aspects. In particular, the critical field of superconductivity is extremely low ($B_c = 5\ \mu$T [7]), much lower than the local field of the nuclei ($B_{\mathrm{loc}} = 34\ \mu$T [8]), which provides the unique possibility to switch between the normal and superconducting phases without disturbing the nuclear spin system.

This thesis presents the results of SQUID-NMR studies of a rhodium single crystal at record low temperatures. In the following sections the cryogenics and the sample properties are first shortly reviewed. The measurement setups and typical measurement

schemes are presented. The main results of the experiments are then described, starting from the susceptibility measurements and the search for the ordered spin state, followed by multiple spin flip resonances, and concluded by the measurements in the superconducting state.

2 Experimental techniques

2.1 Cryogenics

The experiments reported in this thesis were performed in the new YKI-cryostat of the Low Temperature Laboratory. It is a large two-stage nuclear demagnetization cryostat particularly designed for studies of nuclear magnetism at ultralow temperatures [P2]. The layout of the cryostat is shown in Fig. 1.

The precooling unit for the nuclear stages is a commercial dilution refrigerator, providing a large cooling power at millikelvin temperatures for removing the nuclear entropy of the massive first demagnetization stage. In the performance tests the dilution unit reached a base temperature of 3.0 mK, and the cooling power was 10 μW at 10 mK with a circulation of 1500 μmole/s.

The first nuclear stage is manufactured from a high purity copper rod. The total amount of copper is 170 moles, out of which 98 moles is effectively in the 9 T field of the first demagnetization magnet. In order to avoid excessive eddy current heating during the demagnetization, 21 slits were cut by a spark cutter along the long axis of the copper rod. Before installation, the nuclear stage was annealed in a vacuum oven at 960 °C, for 100 h, with 1×10^{-3} mbar of air flowing through during the treatment. The RRR of the copper was 1500 after the annealing.

The copper demagnetization stage is connected to the dilution unit via a superconducting heat switch. The superconducting element of the switch is aluminum, which has, among the suitable metals, the highest ratio of thermal conductivity between the normal and superconducting states. The aluminum foils were connected to the copper pieces by diffusion welding. The total residual resistance of the heat switch is about 100 nΩ, corresponding to a thermal conductance of $0.3\ T$ W/K^2.

The second demagnetization stage is the sample itself. It is connected to the first stage through a solid thermal link made of copper and silver. The second stage is magnetized by a 7.5 T magnet located in vacuum inside the heat exchangers of the dilution unit.

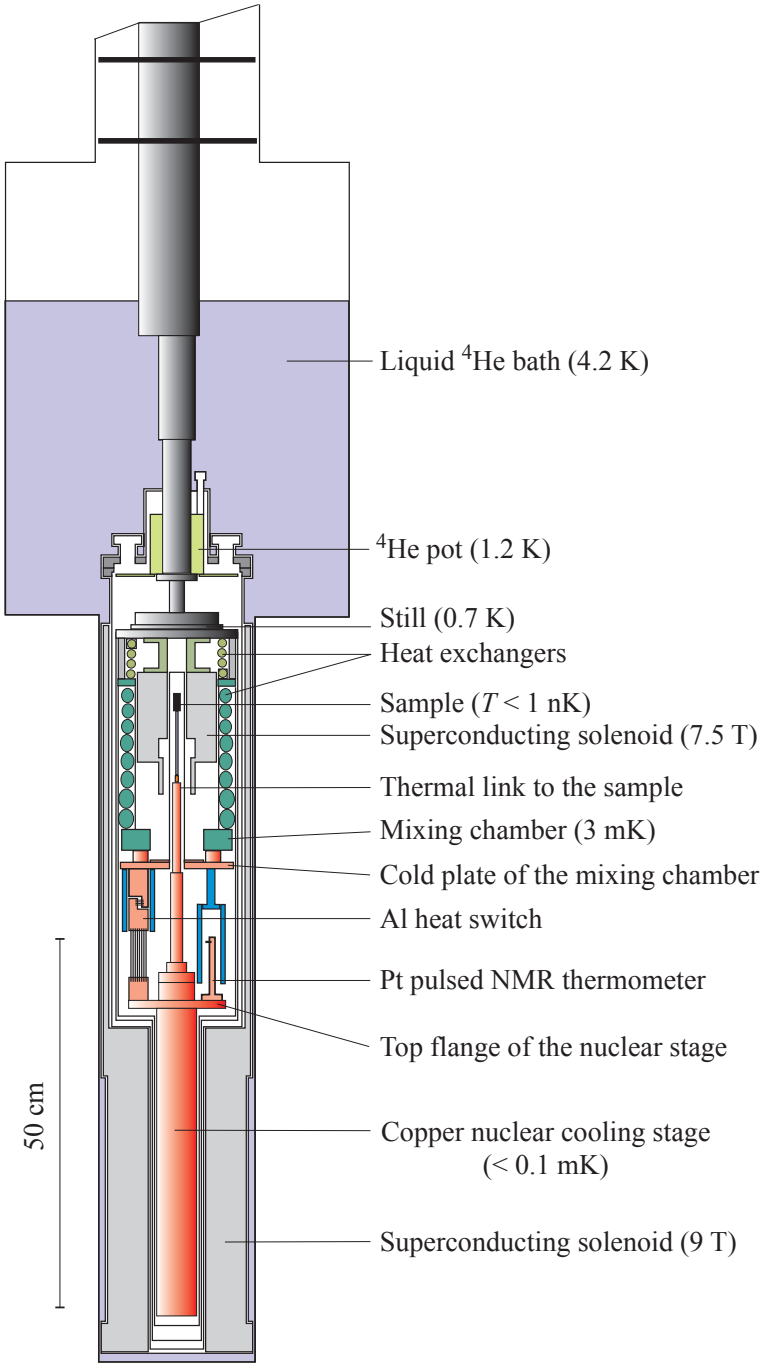

Figure 1: The layout of the cryostat.

Several different thermometric methods were used to monitor the temperature of the cryostat during the performance tests and the experiments. The devices mainly used in the low temperature regime were a vibrating wire thermometer, a nuclear orientation thermometer (NO), a platinum pulsed NMR thermometer, and a Coulomb blockade thermometer. A vibrating wire, placed inside the mixing chamber, measures the temperature of the helium liquid directly and is very useful in diagnosing the performance of a dilution refrigerator. The NO thermometer, a primary device, was employed to calibrate the Pt thermometer and Pt NMR was exclusively used to measure the temperatures below 1 mK. The Coulomb blockade thermometer, using nanoscale tunnel junctions, is a recent development [9]. It can be used either for primary or secondary thermometry and covers a large temperature range from 40 K to 20 mK [P1].

2.2 Rhodium sample

The sample was a slab shaped single crystal of rhodium, with dimensions 0.4 x 5 x 25 mm^3, in the directions x, y and z, respectively. The nominal purity of the sample was 99.99%, with 15 ppm of Fe as the major magnetic impurity.

In order to improve the thermal conductivity and to neutralize magnetic impurities by selective oxidization and precipitation, the sample was heat treated in a low pressure oxygen atmosphere [P3]. The annealing was performed in 0.4 μbar pure O_2, in several steps, first at 1300°C and later at 1530°C. The resulting RRR value was 740 after a total of 380 h of treatment.

The sample was connected to the end of the silver thermal link by diffusion welding. The contact resistance at low temperatures was measured to be 40 nΩ, which is a low value compared with the residual resistance of the rhodium itself, 760 nΩ over the whole length.

To protect the sample from the remnant field of the 7.5 T demagnetization magnet, a cylindrical magnetic shield was manufactured from Cryoperm-10 [10], a high permeability material designed for low temperatures, and installed around the sample. The low temperature shielding factor was more than 1000 and the shield saturated in a field of about 10 mT.

2.3 NMR setup and measurements

Due to the very small magnetic moment of the nuclei, the measurements were performed by low-frequency SQUID-NMR between 3 and 1000 Hz. Two different pick-up coil arrangements were used during the course of the experiments [P8]. The coil systems included pick-up and excitation coils and three static coils, in the spatial directions x, y and z. The pick-up coil was connected to a dc-SQUID for recording the signal.

The first half of the measurements was performed with a coil system wound solely of thin 50 μm superconducting wire. The pick-up coil was a planar second-order gradiometer, which had two loops around the sample and single compensation loops on both sides of the sample. Such a design has several benefits, as it eliminates both uniform and gradient disturbances and could be placed close to the sample giving a good filling factor. The pick-up coil gave a clean and noise-free signal.

The superconducting coil system, however, sustained a trapped flux of the order of a few μT, which prevented the detection of the superconducting transition of the Rh-sample. To avoid this problem and enable the superconducting transition, a second coil system was installed for the latter half of the measurements. The second coil system consisted mostly of copper wire and only the two static saddle coils in the x and y-directions were made of the superconducting wire. The pick-up coil in this setup was a conventional axial astatic pair with 4+4 turns, wound of 0.5 mm Cu-wire.

The collected data consist mainly of the NMR peaks measured in a small external field and of a low frequency response at 3 Hz measured at zero external field. The zero field absorption maximum of rhodium is at about 50 Hz [8], so the response at 3 Hz is almost purely dispersive, giving essentially the static susceptibility $\chi'(0)$. The NMR lineshapes in an external field were measured by sweeping the magnetic field, while the excitation frequency was constant. The excitation frequency was typically 431 Hz and the field was swept between 200 and 440 μT. The spectra were fitted to Lorentzian lineshapes with a free phase factor and background. The area of the absorption signal, a measure of the nuclear polarization, was deduced analytically from the fit parameters.

3 Results

3.1 Susceptibility measurements

The static susceptibility is a central quantity in these experiments. An antiferromagnetically ordered nuclear spin system should produce a saturation of the susceptibility, which is easy to observe. The static susceptibility as a function of nuclear temperature can readily be compared with the Curie-Weiss law, which gives general information about the nature of the mutual interactions between the spins and an order of magnitude estimate for the expected ordering temperature.

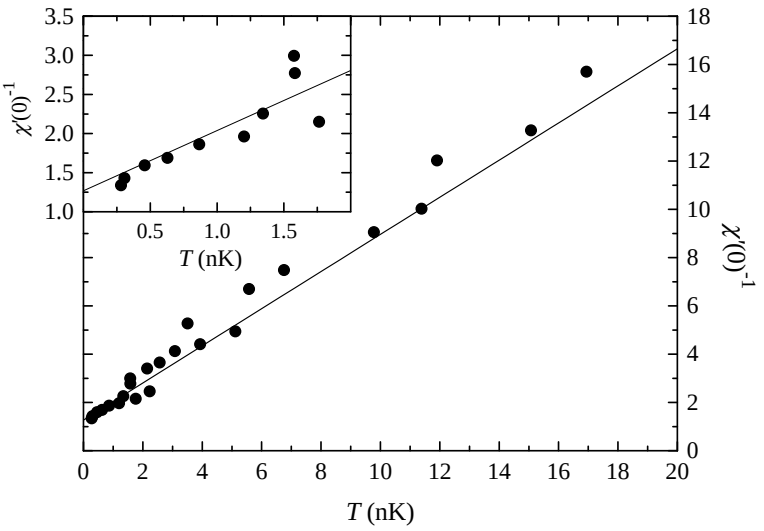

Figure 2: Inverse static susceptibility vs. nuclear temperature. The solid line is a fit of the antiferromagnetic Curie-Weiss law with $\lambda = 1.3$ nK and $\theta = -1.65$ nK. The inset shows a close-up of the low temperature end.

Figure 2 shows the inverse static susceptibility as a function of nuclear temperature T. The temperature of the spin system was determined using the well established method based on the second law of thermodynamics [P8]. The Curie-Weiss law,

$$\chi'(0) = \frac{\lambda}{T - \theta}, \tag{1}$$

was fitted to the data, with θ as the only free parameter. This gives $\theta = -1.65$ nK. The behavior thus clearly indicates a tendency for antiferromagnetic ordering of the spin system.

The magnetically ordered state of the nuclei was searched for by monitoring the low-frequency 3 Hz signal in several runs with high initial polarizations after demagnetizing

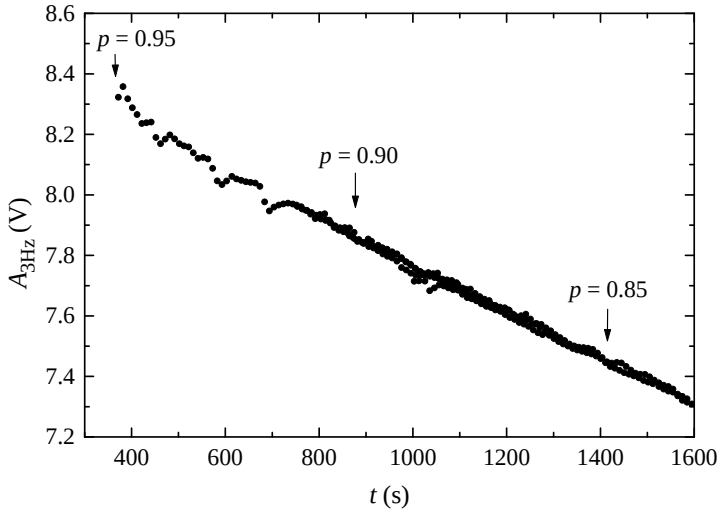

Figure 3: Static susceptibility, in arbitrary units, vs. time while the nuclei warm up after the end of the demagnetization. Several runs are shown, with different initial polarizations. The runs with lower initial polarization have been shifted in time to coincide with the best one. The polarization values were deduced from a separately measured curve of static susceptibility vs. polarization.

to a low field. The highest initial polarizations reached were $p = 0.95$, i.e. clearly higher than the 0.83 obtained earlier by Hakonen *et al.* [8] and much higher than required for ordering of Cu ($p_c = 0.74$) or Ag ($p_c = 0.67$) [2, 3], where the mutual interactions are of the same order of magnitude. Nevertheless, no features attributable to magnetic ordering were observed. The data from a few of such runs are shown in Fig. 3. The signal is relaxing monotonously from the very beginning without the anticipated initial saturation or increase.

3.2 Multiple spin flips

The dipolar coupling between the nuclei allows a single photon to flip two or more spins simultaneously, giving rise to resonances at integer multiples, harmonics, of the Larmor frequency, $f_0 = \gamma B/2\pi$. These higher order resonance lines yield direct information about the mutual coupling of the spins. In particular, the frequency shift of the double-spin flip resonance at high nuclear polarization gives selectively the magnitude of the isotropic indirect-exchange interaction [11, 12].

The double-spin flip resonance in rhodium was observed in these experiments both at positive and negative spin temperatures [P4, P6]. The existence of the multiple spin

flips is perhaps best demonstrated by the use of a parallel field NMR geometry, where the static and excitation fields are applied parallel to each other. In such a geometry, the main Larmor resonance also originates by the dipolar coupling and thus has an intensity comparable with the double-spin flip peak [13, 14]. In the conventional orthogonal-field NMR geometry the multiple spin-flip resonances have a much weaker intensity compared to the main Larmor line and are easily obscured by it.

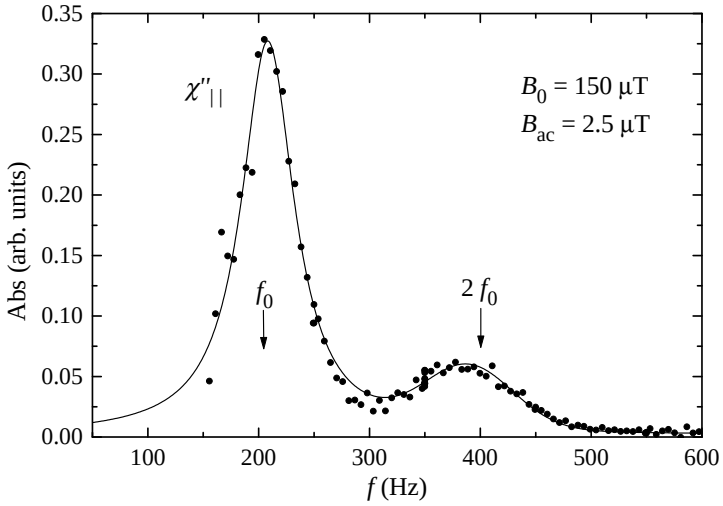

Figure 4: Parallel field absorption showing the Larmor and double-spin flip resonances. The data were measured at a field of 150 μT. f_0 and $2f_0$ mark the exact Larmor and double-Larmor positions, while the actual resonances are shifted due to the mutual interactions. The solid line shows a fit with a Lorentzian lineshape for the main peak and a Gaussian for the double-flip peak.

The absorption peaks in Fig. 4 were measured by monitoring the decay of a low frequency susceptibility signal during a frequency sweep of a larger ac-excitation $B_{\rm ac}$ along the static field B_0. The low frequency signal at 8 Hz is essentially proportional to nuclear polarization and the ac-excitation level was adjusted to cause a substantial decrease of the polarization at the absorption maxima. Absorption in arbitrary units can then be calculated as the normalized time derivative of the low-frequency signal, $(\mathrm{d}\chi_{8\mathrm{Hz}}/\mathrm{d}t)/\chi_{8\mathrm{Hz}}$. This method has the advantages that it is sensitive exclusively to the absorption part and has an essentially zero baseline. The resolution of the measurement was good enough to allow to state that the main peak is Lorentzian in shape, while the double-spin flip peak is Gaussian.

The frequency shifts of the resonance lines were, however, quantitatively analyzed

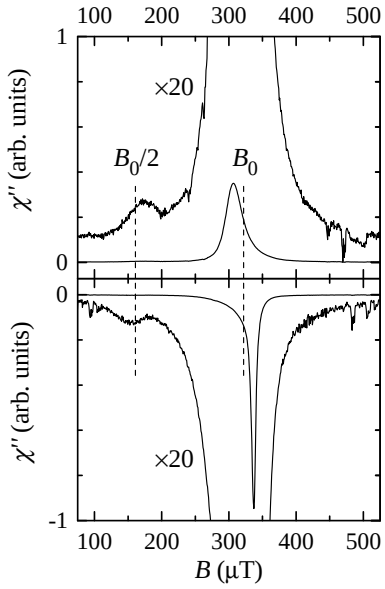

Figure 5: Double-spin flip peak at $p = 0.39$ (top frame) and at $p = -0.39$ (bottom frame), with $f = 431$ Hz. The double-spin flip satellite becomes clearly visible, when the data are magnified by a factor of 20. The resonances are slightly shifted from the exact Larmor and double-Larmor positions, shown by the dashed lines.

only for the conventional orthogonal-field NMR geometry, as it allows for much faster measurements. An example of the resonance lines, both at positive and negative temperatures, are shown in Fig. 5. The shifts from the pure Larmor and double-Larmor values are clear, and as expected, the shifts are in opposite directions at positive versus negative temperatures.

The double-spin flip mode was observable with frequencies from 131 to 831 Hz. At lower frequencies the satellite was obscured by the main line and at higher frequencies the intensity, behaving as $1/f^2$, became too weak to be observed. The behavior of the satellite resonance was investigated with polarizations ranging from -0.45 to 0.81.

The essential observables in these experiments are the resonance frequencies of the Larmor and double-spin flip modes. From the shifts of these frequencies, the dipolar-like contribution and the isotropic exchange term can be separately deduced, as the exchange term does not shift the main line, but does influence the double-spin flip mode. The

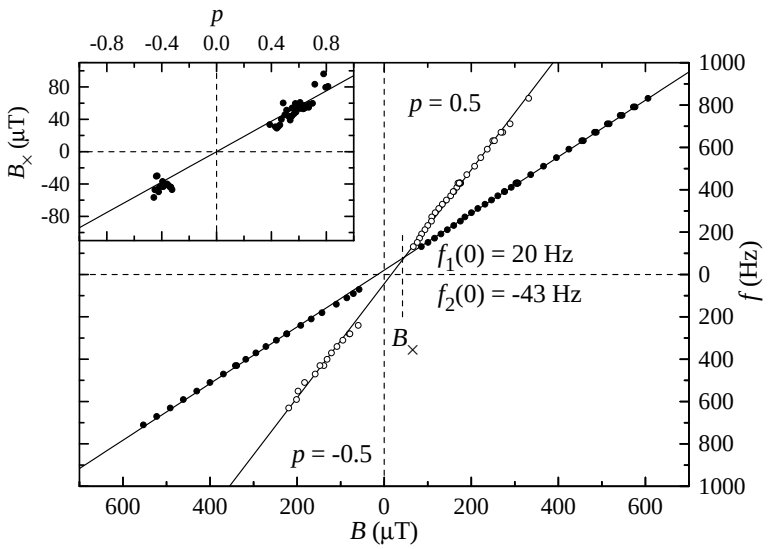

Figure 6: Resonance frequencies of the Larmor and double-spin flip modes as a function of magnetic field. The data are reduced to $|p| = 0.50$. The solid lines show linear fits with the slopes μ/Ih and $2\mu/Ih$, while the shifts from the origin, $f_1(0)$ and $f_2(0)$, are due to the dipolar and exchange interactions between the spins. The inset shows the line crossing field $B_\times$ of the two resonances as a function of polarization.

resonance of the coupled Larmor and double-spin flip lines are given by [11, 12]

$$f_1 = f_0 + \tfrac{1}{2}(1 - 3D)f_s p, \tag{2}$$

$$f_2 = 2f_0 + 2(R + \tfrac{1}{3} - D)f_s p, \tag{3}$$

where D is the demagnetization factor along the static field in the plane of the sample and $R = \Sigma_j J_{ij} I/hf_s$ is the relative exchange parameter. $f_s = \mu_0\mu^2\rho/Ih + f_{\rm ae}$ is the "dipolar frequency", where ρ is the atom number density and $f_{\rm ae}$ the anisotropic exchange contribution. Because of the polarization dependent frequency shifts, the two modes appear to cross at a nonzero field value

$$B_\times = -(2R + \tfrac{1}{6} - \tfrac{1}{2}D)Ihf_s p/\mu. \tag{4}$$

In Fig. 6 an excitation frequency versus resonance field plot has been compiled, where the p-dependence is reduced to $|p| = 0.5$. Linear fits to the Larmor and double-spin resonance frequencies with slopes μ/Ih and $2\mu/Ih$, respectively, give the offsets $f_1(0) = 20 \pm 1$ Hz and $f_2(0) = -43 \pm 2$ Hz at $B = 0$, where $f_0 = 0$. In the inset of Fig. 6, the polarization dependence of the line crossing field $B_\times$ is shown. The linear behavior, as expected from Eq. 4, is well obeyed.

Including the minor effects of eddy currents and of the finite demagnetization factor $D = 0.08$ ($B \parallel y$), the values $R = -0.9 \pm 0.1$ and $f_s = 74 \pm 6$ Hz are obtained from the above given shifts of the resonance lines. The pure dipolar interaction in rhodium would give $f_s = 54$ Hz, and the additional shift is attributed to the anisotropic indirect exchange term $f_{\rm ae} = 20 \pm 6$ Hz [15]. If the isotropic exchange is compared with the actual dipolar interaction alone, i.e. $R = \Sigma_j J_{ij} I^2/\mu_0\mu^2\rho$, one obtains $R = -1.2$, which agrees rather well with the value $R = -1.35$ adopted by Hakonen *et al.* [8].

3.3 Superconducting state

The superconducting transition of the rhodium sample was finally detected with the Cu-wire pick-up system (see Section 2.3) [P5, P8]. The supercooling was very strong and the transition to the superconducting state was possible only at fields below 0.25 μT.

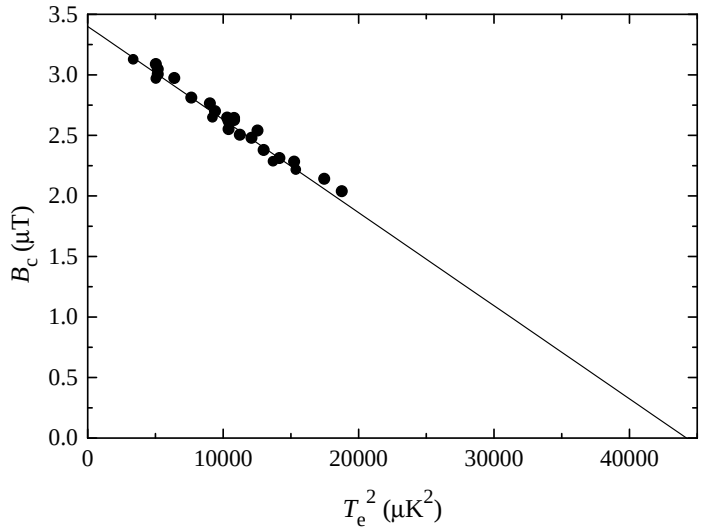

Figure 7: Critical field vs. temperature squared. The fitted line can be extrapolated to yield T_c and B_c.

The critical field B_c of the transition was measured by sweeping the z-direction static coil at a constant electronic temperature. The lowest lattice temperature achieved was $T_e = 60$ μK and the transition could be traced up to 140 μK, after which the supercooling prevented the occurrence of the transition. The temperature dependence of the critical field is shown in Fig. 7. Extrapolating the data, by fitting the form $B_c(T_e)/B_c(0) = 1 - (T_e/T_c)^2$, one obtains the critical parameters $B_c(0) = 3.4$ μT and $T_c = 210$ μK. These are somewhat lower values than obtained earlier by Buchal *et al.*, $B_c(0) = 4.9$ μT

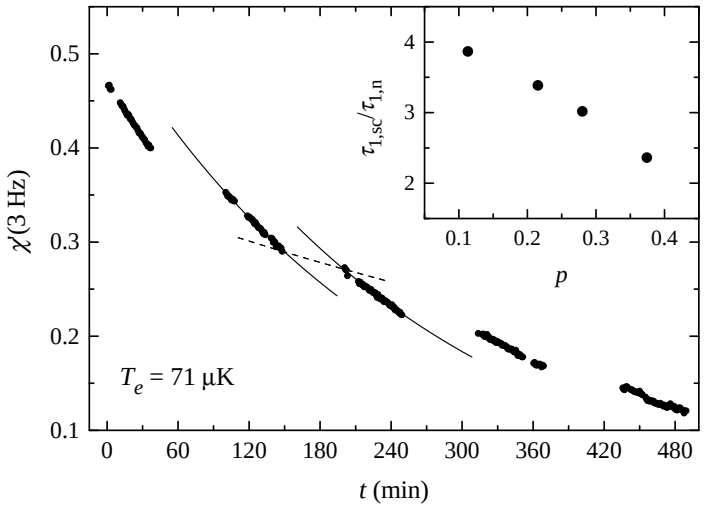

Figure 8: Data from a relaxation rate measurement at $T_e = 71$ μK and $p_i = 0.55$. The 3 Hz susceptibility as a function of time is shown. The data are measured in the normal state, whereas during the large gaps the sample is in the superconducting state. The solid lines show exponential fits to the normal state data, while the dashed line shows the interpolation for the relaxation in the superconducting state. The small gaps in the data are caused by unlocking of the dc-SQUID. The inset shows the ratio of the relaxation times as a function of polarization.

and $T_c = 325$ μK [7]. However, the residual resistivity of our sample was higher, 740, as compared to the value of 450 of the cleanest sample of Buchal *et al.*, which would indicate that the purity of our sample was better. This apparent discrepancy can be at least qualitatively explained by the compensation of the paramagnetic-impurity effect by ordinary, nonmagnetic impurities [16], i.e., the suppression of the critical parameters by paramagnetic impurities is reduced by the presence of nonmagnetic impurities.

The critical field of Rh is exceptionally low, and particularly, it is much lower than the internal local field of the nuclei. Thus, as the short range spin-spin interactions are expected to remain unchanged in the superconducting transition, it should be possible to switch the electron system between the normal and superconducting states without disturbing the nuclear spins.

The nuclear polarization did remain unchanged, when switching the sample with polarized nuclei repeatedly between the normal and superconducting states, which verifies that the transition itself did not effect the spin system. This provides the possibility to measure the spin lattice relaxation time in both the normal and superconducting states by simply monitoring the relaxation of the nuclear polarization [P7, P8].

The nuclei could be polarized in a field of only 2 T, as higher field values increased the remanence field after demagnetization and the superconducting transition could no longer be detected. Therefore, the highest initial nuclear polarizations were $p = 0.55$.

A typical measurement of the spin lattice relaxation is presented in Fig. 8. The ac-susceptibility at a frequency of 3 Hz is monitored, while the sample is alternatively in the normal and superconducting states. The switching between the normal and superconducting states was done by minute changes of the external magnetic field. In the superconducting state the response of the spins cannot be seen because of the Meissner-effect, but the relaxation can be interpolated from the normal state signals. At the investigated range $p \leq 0.55$, the signal is practically proportional to the polarization, $\chi'(3Hz) \approx 0.9\ p$. The ratio $\tau_{1,\mathrm{sc}}/\tau_{1,\mathrm{n}}$ is plotted in the inset of Fig. 8. It shows a strong dependence on nuclear polarization (or susceptibility), which cannot be accounted for by simple arguments.

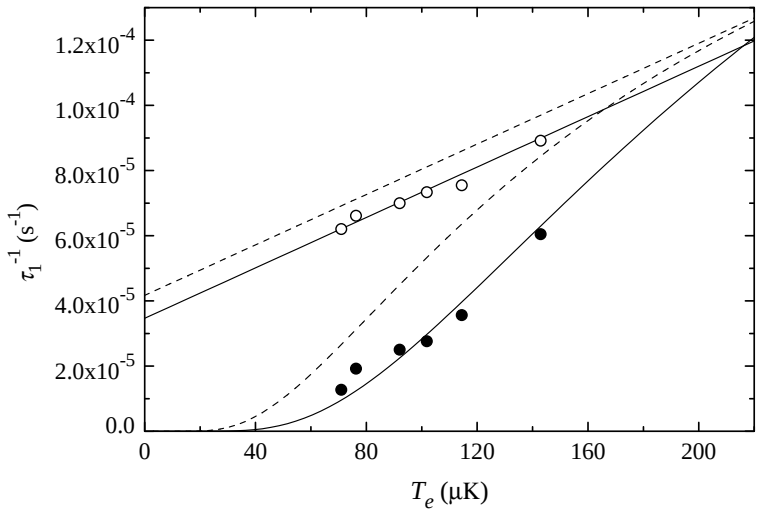

Figure 9: The reciprocal of the spin lattice relaxation time in the normal (open points) and superconducting (closed points) states as a function of electronic temperature at the limit $p = 0$. The solid lines show a linear and an exponential fit to the data, whereas the dashed lines show the observed behavior at $p = 0.5$. The data points at finite nuclear polarizations have been omitted.

Such measurements were performed at several electronic temperatures and the results after the analysis are presented in Fig. 9. For a meaningful comparison the relaxation rates (reciprocal spin lattice relaxation times) have been extrapolated to the limit of zero nuclear polarization. The normal state data follows very well the expected linear

behavior given by the Korringa law. The data, however, has a clear offset, which can be attributed to paramagnetic impurities. According to the BCS-theory, the superconducting state relaxation rate should first display a coherence enhancement just below T_c and then follow an exponential behavior, $\propto e^{-\Delta/k_BT}$ [4, 17]. The data do not indicate any coherence enhancement, but do fit well an exponential curve. The fitting, however, gives $\Delta/k_BT_c = 0.79$, whereas the BCS-value is 1.76. It is also noteworthy that the zero temperature offset observed in the normal state rate is completely absent in the superconducting state.

The suppression of the coherence enhancement and the low gap value Δ can result from the presence of electronic paramagnetic impurities [17, 18]. A comparison with existing theoretical work would then imply a true T_c of about 0.5 mK for pure Rh [19]. This agrees well with the conclusions of Buchal *et al.*, who also state that the T_c of pure rhodium could be about 0.5 mK [7]. A suppression of T_c by $\sim 200 - 300$ μK can be produced by a minute active paramagnetic impurity concentration of the order of 1 ppm.

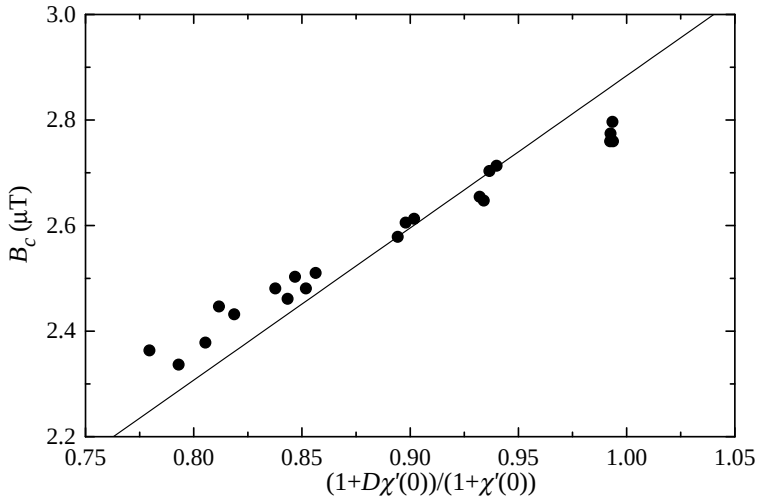

Figure 10: The influence of nuclear static susceptibility on the critical field of the superconducting transition. The x-axis was chosen so that the behavior should be linear and intersect the origin as shown by the solid line, see the text. The electronic temperature during the measurement was 89 μK.

Nonzero nuclear magnetization affects the superconducting state as it modifies the magnetic field inside the sample. This was studied by measuring the critical field of the transition as a function of nuclear static susceptibility. The expected behavior can be deduced from the basic equations of electromagnetism leading to $B_c(\chi) = B_c(\chi{=}0)(1 + D\chi)/(1 + \chi)$. The demagnetization factor was $D = 0.01$ as the transitions were measured

along the z-axis. The measured data are shown in Fig. 10.

4 Conclusions

This thesis presents the results of the second set of experiments at the Low Temperature Laboratory in Helsinki studying the nuclear spin system of rhodium at ultralow temperatures with both positive and negative nuclear polarizations. The experiments were performed with the new cooling apparatus particularly designed for such measurements. These measurements were extended to a completely new regime, where polarized nuclei were embedded in a coherent superconducting conduction electron system.

The highest nuclear polarizations reached at positive temperatures were $p = 0.95$, i.e., considerably higher than the value $p = 0.83$ reached in the earlier experiments [8]. The quality of the sample was also very good, as indicated by the zero field spin lattice relaxation time, which was nearly an order of magnitude longer as compared to the earlier samples. The measured data showed a clear antiferromagnetic tendency, but no indications of actual nuclear magnetic ordering were observed. On the temperature scale the highest initial polarizations correspond to nuclear spin temperatures below 100 pK, which is an order of magnitude lower than the fluctuation corrected theoretical Néel temperature of 1 nK for an antiferromagnetic structure [20]. The disagreement between experimental and theoretical results, which surfaced already during the earlier set of experiments by Hakonen *et al.*, thus still remains an open question. Of course, the possibility that the nuclear susceptibility signal just did not display the characteristic anomalies in the experiments, cannot be completely ruled out.

Multiple spin flips, where a single photon flips several nuclei were observed in rhodium for the first time. Uniquely the double spin flip resonance was observed also at negative spin temperatures. The frequency shift of the double-spin flip peak gave a direct measure for the mutual interactions between the nuclear spins, which gives a good basis for eventual theoretical studies.

Because of the rare properties of Rh, where the critical field of superconductivity is considerably lower than the local field of the nuclei, experiments could be carried out with polarized nuclei also in the superconducting state of the electron system. The results of these measurements rose new and intriguing questions about the interaction of nuclear magnetism and superconductivity. The observed spin lattice relaxation time was longer in the superconducting state as compared to the normal state, as is expected

from the BCS-theory at $T_e \ll T_c$. However, no signs were observed of the BCS coherence enhancement near the critical temperature, where the relaxation time should be shorter in the superconducting state. The spin lattice relaxation in the superconducting state showed a strong dependence on nuclear polarization, which cannot be explained by simple arguments.

5 Publications

This thesis is based on the following original publications.

P1. T. A. Knuuttila, K. K. Nummila, W. Yao, J. P. Kauppinen, and J. P. Pekola, *Direct Measurements of Electron Thermalization in Coulomb Blockade Nanothermometers at Millikelvin Temperatures*, Physica E **3**, 224 (1998).

Electron thermalization of tunnel junction arrays in the millikelvin temperature range was studied. The behavior of the Coulomb blockade thermometer (CBT), which can be used as a primary or secondary thermometer, was compared against other thermometers in the YKI cryostat. The direct heat leak limited the minimum electronic temperature of the CBT to slightly below 20 mK. The contributions to the heat leak from the wiring and the bias current were investigated.

P2. W. Yao, T. A. Knuuttila, K. K. Nummila, J. E. Martikainen, A. S. Oja, and O. V. Lounasmaa, *A Versatile Nuclear Demagnetization Cryostat for Ultralow Temperature Research*, J. Low Temp. Phys. **120**, 121 (2000).

The design and structure of the new YKI double-stage nuclear demagnetization cryostat and its peripherals are described in detail. Results of the performance tests are presented.

P3. K. Lefmann, T. A. Knuuttila, J. E. Martikainen, L. T. Kuhn, and K. K. Nummila, *Effect of Heat Treatment of Pure and Carbon-polluted rhodium Samples on the Low-temperature Resistivity*, J. Mater. Sci. **36**, 839 (2001).

A systematic investigation of optimal conditions for heat treatment of Rh with the aim of increasing the residual resistivity ratio (RRR) is presented. The maximum value of $RRR = 1050$ was reached in a thin foil sample annealed at $T = 1500$°C and a low pressure of oxygen, around 1 μbar.

P4. J. T. Tuoriniemi, T. A. Knuuttila, K. Lefmann, K. K. Nummila, W. Yao, and F. B. Rasmussen, *Double-Spin Flip Resonance of Rhodium Nuclei at Positive and Negative Spin Temperatures*, Phys. Rev. Lett. **84**, 370 (2000).

The double-spin flip resonance rising from the dipolar coupling was observed in rhodium

at both positive and negative spin temperatures. The measured frequency shifts of the resonance lines allow deducing the strength of the dipolar-like and isotropic exchange terms. The value $R = -0.9 \pm 0.1$ is obtained for the isotropic exchange. Also the intensity of the double-spin flip resonance was studied.

P5. J. T. Tuoriniemi and T. A. Knuuttila, *Nuclear Cooling and Spin Properties of Rhodium down to Picokelvin Temperatures*, Physica B **280**, 474 (2000).

The nuclear spin properties of rhodium are shortly reviewed and compared with those of copper and silver. The SQUID-NMR measurement techniques are discussed. Some results of the susceptibility measurements in rhodium are presented. The observation of the superconducting transition in the sample is reported.

P6. T. A. Knuuttila, J. E. Martikainen, F. B. Rasmussen, and J. T. Tuoriniemi, *Double Spin Flip Mode of Rhodium Nuclei*, Physica B **284**, 1700 (2000).

The results of the double-spin flip resonance experiments are presented in a condensed form.

P7. T. A. Knuuttila, J. T. Tuoriniemi, and K. Lefmann, *Relaxation of Polarized Nuclei in Superconducting Rhodium*, Phys. Rev. Lett. **85**, 2573 (2000).

Nuclear spin lattice relaxation times were measured with polarized nuclei both in the normal and superconducting states. The highest nuclear polarizations reached were $p = 0.55$. Because in rhodium $B_c \ll B_{\mathrm{loc}}$, and the short-range spin-spin interaction is unchanged, the transition between the normal and superconducting states was adiabatic. The relaxation times were always longer in the superconducting state and no signs of the coherence enhancement of the relaxation close to T_c were seen. Non-zero nuclear polarization was observed to reduce the difference between the relaxation rates in the normal and superconducting states.

P8. T. A. Knuuttila, J. T. Tuoriniemi, K. Lefmann, K. I. Juntunen, F. B. Rasmussen, and K. K. Nummila, *Polarized Nuclei in Normal and Superconducting Rhodium*, Report TKK-KYL-002 (2000).

A more comprehensive account of the experiments on rhodium is given, with a detailed discussion of the experimental setup. The determination of the nuclear temperature scale

is shown. The results of the susceptibility and spin lattice relaxation time measurements are presented. The evidence for a triple-spin flip peak is reported.

The author's own contribution:

The research work presented in this thesis is a result of team work.

Starting from 1993 as a junior member, I participated in all phases of the designing, constructing and testing of the new nuclear demagnetization cryostat. I had a major responsibility of the day-to-day operations and maintenance of the cryostat from the beginning of 1997 to the beginning of 2000. Most of the presented measurements and the data analysis were done by me.

The measurements for publication P1 were done by me and I wrote most of the text. I was mainly liable for the writing of publications P6, P7, and P8.

Acknowledgments

The experimental work described in this thesis was done in the Low Temperature Laboratory of Helsinki University of Technology.

I wish to express my gratitude to Prof. Mikko Paalanen, the director of the Low Temperature Laboratory, for support and encouragement during my work. I also want to thank the former director, Prof. Olli Lounasmaa, who originally offered me the possibility to participate in low temperature research.

I am especially grateful to my supervisor Dr. Juha Tuoriniemi for his guidance, expertise, and supporting enthusiasm. I am deeply indebted to my other co-workers in the YKI-group; Juha Martikainen, Kirsi Juntunen and Elias Pentti, as well as to our invaluable visitors Kim Lefmann and Finn Rasmussen. I also wish to express my gratitude to all other colleagues who have participated in the work of the YKI-group; Docent Kaj Nummila, Research Prof. Aarne Oja, Prof. Pertti Hakonen, Dr. Reko Vuorinen, Dr. Weijun Yao, Dr. Juha Korhonen, and Teemu Pohjola.

I wish to thank my colleague graduate students, Rob Blaauwgeers, Juha Kopu, Jari Penttilä, Leif Roschier, Jaakko Ruohio, Roch Schanen, and Viktor Tsepelin for providing excellent company during the sometimes rather long working hours. I have also benefited from discussions with Dr. Harry Alles, Dr. Alosha Babkin, Dr. Peter Berglund, Dr. Jaakko Koivuniemi, Academy Prof. Matti Krusius, Dr. Ülo Parts, Docent Erkki Thuneberg, and Dr. Giorgi Tvalashvili.

I am grateful to the administrative staff Teija Halme, Marja Holmström, Pirjo Kinanen, Tuire Koivisto, Satu Pakarinen and Liisi Pasanen with their help in practical matters. I owe much to Antti Huvila, Arvi Isomäki and Antero Salminen for delivering the endless liters of liquid helium consumed during these experiments, and to the skillful machinists of the workshop Juhani Kaasinen, Seppo Kaivola, Hannu Kaukelin, Markku Korhonen, Sami Lehtovuori, and Kari Rauhala, who made the construction of the new cryostat possible.

The whole staff of the Low Temperature Laboratory is thanked for a friendly and inspiring atmosphere.

Otaniemi, August 2000

Tauno Knuuttila

References

[1] A. Abragam and M. Goldman, *Nuclear Magnetism: Order and Disorder* (Clarendon Press, Oxford, 1982).

[2] M. T. Huiku and M. T. Loponen, *Phys. Rev. Lett.* **49**, 1288 (1982).

[3] P. J. Hakonen, S. Yin, and K. K. Nummila, *Europhys. Lett.* **15**, 677 (1991).

[4] L. C. Hebel and C. P. Slichter, *Phys. Rev.* **113**, 1504 (1959).

[5] S. Rehmann, T. Herrmannsdörfer, and F. Pobell, *Phys. Rev. Lett.* **78**, 1122 (1997).

[6] M. Seibold, T. Herrmannsdörfer, and F. Pobell, *J. Low Temp. Phys.* **110**, 363 (1998).

[7] Ch. Buchal, F. Pobell, R. M. Mueller, M. Kubota, and J. R. Owers-Bradley, *Phys. Rev. Lett.* **50**, 64 (1983).

[8] P. J. Hakonen, R. T. Vuorinen, and J. E. Martikainen, *Phys. Rev. Lett.* **70**, 2818 (1993).

[9] J. P. Pekola, K. P. Hirvi, J. P. Kauppinen, and M. A. Paalanen, *Phys. Rev. Lett.* **73**, 2903 (1994).

[10] Vacuumschmelze GmbH, Grüner Weg 37, 63450, Hanau, Germany.

[11] J. P. Ekström, J. F. Jacquinot, M. T. Loponen, J. K. Soini, and P. Kumar, *Physica* **98B**, 45 (1979).

[12] P. L. Moyland, P. Kumar, J. Xu, and Y. Takano, *Phys. Rev. B* **48**, 14020 (1993).

[13] H. Cheng, *Phys. Rev.* **124**, 1359 (1961).

[14] A. G. Anderson, *Phys. Rev.* **115**, 863 (1959).

[15] A. Narath, A. T. Fromhold, Jr, and E. D. Jones, *Phys. Rev.* **144**, 428 (1966).

[16] Yong-Jihn Kim and A. W. Overhauser, *Phys. Rev. B* **49**, 15799 (1994).

[17] D. E. MacLaughlin, in *Solid State Physics,* edited by H. Ehrenreich, F. Seitz, and D. Turnbull, volume 31 (Academic, New York, 1976).

[18] A. Griffin and V. Ambegaokar, In *Proc. Int. Conf. Low Temp. Phys., 9th, Columbus, Ohio, 1964,* edited by by J. G. Daunt, D. O. Edwards, F. J. Milford, and M. Yaqub, (Plenum, New York, 1965).

[19] A. A. Abrikosov and L. P. Gor'kov, *JETP* **12**, 1243 (1961).

[20] A. S Oja and O. V. Lounasmaa, *Rev. Mod. Phys.* **69**, 1 (1997).